Herd Behavior Is Sufficient to Reproduce Human Evacuation Decisions During the Great East Japan Earthquake

Akira Tsurushima[(⊠)] [ID]

SECOM CO., LTD., Intelligent Systems Laboratory, Tokyo, Japan
`a-tsurushima@secom.co.jp`

Abstract. We previously developed an evacuation decision model to represent the herd behaviors of evacuees during a disaster evacuation and employed it to analyze symmetry breaking in evacuation exit choice, a phenomenon in which people tend to gather at one specific exit during an evacuation. This model had yet to be tested against real disaster data owing to a difficulty in acquiring such data. An analysis of video clips captured during the Great East Japan Earthquake revealed unusual evacuation behaviors of people in a meeting room, namely, the evacuation decision between fleeing and drop, cover, and hold-on actions depending on the distance from the exit. Such behaviors have yet to be reported in the literature. We conducted simulations and reproduced these evacuation behaviors using an evacuation decision model and determined that simple herd behaviors among evacuees are sufficient to reproduce these unusual evacuation behaviors. We also conducted logistic-regression, graph-centrality, and sensitivity analyses to examine the nature of these simulation results.

Keywords: Evacuation behavior · Herd behavior · Decision-making · Video analysis · Response threshold model

1 Introduction

Cognitive biases, i.e., mental inclinations used to derive irrational decisions or erroneous behaviors, during disaster evacuation situations have received the attention of numerous researchers and experts owing to their serious effect on the evacuation results, including a loss of life. Herd behavior is one of the most typical cognitive biases of this type [7, 10]. During herd behavior, people make decisions not by themselves but based on the decisions of other people, and this behavior sometimes incurs unusual phenomena, particularly during crowd evacuations. The symmetry breaking in exit choice has become a well-studied example of unusual phenomena caused by herd behavior during crowd evacuations [1, 27].

When a group of people attempt to evacuate an environment with multiple exits, the exits are often used unevenly, and people tend to gather at one specific exit. This phenomenon of symmetry breaking in exit choice is considered irrational because the expected evacuation time will be the shortest, meaning a safe evacuation will be achieved if these exits are used evenly. We developed and proposed an evacuation decision model [25] to represent human herd behaviors during the evacuation processes,

and we employed it to analyze the symmetry breaking in evacuation exit choices. The evacuation decision model revealed that simple herd behaviors are sufficient to reproduce a symmetry breaking in exit choice, and that no intentional or rational decisions are required for this phenomenon to emerge [27].

Research on human behaviors during a disaster evacuation has been primarily conducted through interviews [9,19], laboratory experiments using human subjects [11,22], and laboratory experiments using nonhuman animals [1,21]. However, these techniques are limited for the following reasons:

1. interviews can only be conducted with survivors,
2. it is difficult to reproduce the mental pressure of real evacuations in laboratory experiments, and
3. animal behaviors are not necessarily identical to human behaviors.

None of the above aspects provide assurance that the data obtained through these methods refer to real human behaviors during a disaster situation.

Like many other phenomena regarding disaster evacuations, the symmetry breaking in exit choice has been studied through these methods because no numerical data are available owing to the difficulty of gathering such data during a real situation. Additionally, data for disaster evacuations are only available for certain global cases such as the evacuation time and the number of evacuees of specific groups. Thus, we reproduced the symmetry breaking phenomenon in a qualitative sense, although these results have yet to be validated against objective data owing to the absence of real data.

In constructive approaches for human behaviors during disaster evacuations, including our studies, model validation is crucial but difficult owing to the limited amount of objective data. Hence, data for human evacuations, which are both objective and numeric, are extremely valuable in this sense. With an increase in the numbers of surveillance cameras and smartphones, video images of human behavior during disasters have been recorded. These videos have recently been analyzed, and human evacuation behaviors have been investigated [8,12,15,30]. However, problems such as accessibility and poor video quality have limited the success of these approaches [23].

A video clip captured in a meeting room in Sendai during the Great East Japan Earthquake of March 11, 2011 (Fig. 1), is exceptionally valuable for the following reasons:

– the earthquake was captured in one continuous scene from beginning to end,
– the initial positions of the people in the room when the shaking began were clearly recorded, and
– the professionalism of the camera crew rendered it relatively easy to examine the behavior of every individual during the earthquake.

By studying this video, real human behaviors during an earthquake can be analyzed.

In a previous study, we analyzed the behavior of individuals in this video and found unusual human evacuation behaviors that had yet to be reported in the literature. We also attempted to reproduce this real human evacuation behavior using the evacuation decision model for validation purposes and revealed that a simple herd behavior is sufficient to reproduce such behavior [28].

This paper extends our previous research in two ways. First, we conducted 500 simulations rather than 150 simulations to obtain more accurate results, and the results in Sect. 5.3 are replaced by new data that had been acquired through these simulations. Second, we conducted two more analyses to examine the nature of the simulation model and its results. A graph centrality analysis is conducted to investigate the influence dynamics among agents during the evacuation processes. The influence between two decisions of the agents produces a complex network, and the relations of the agents within the network are analyzed through graph centralities. Moreover, the sensitivities of the parameters of the evacuation decision model are analyzed. Because the population density and defined vicinity of an agent are two influential factors affecting herd behaviors, we conducted a sensitivity analysis for agent population densities and a variety of agent vicinities. These analyses are given in Sects. 6.2 and 6.3, respectively.

2   Related Studies

Since it was difficult to obtain objective data, research on human behaviors during earthquake evacuations have been conducted primarily through interviews, case studies using surveys, or experiments using animals or humans. The subjects of case studies include the 2004 Mid-Niigata prefecture earthquake [17], 2010 Chile earthquake [9], and Great East Japan Earthquake [20]. Herein, we investigated the behavioral and psychological reconstruction processes for the victims [17], distributions of departure times of tsunami evacuations [19], solidarity behaviors, and pre-/post- earthquake evacuation behaviors [9, 20]. Several studies have been conducted on human and animal evacuation experiments such as [3, 13, 14, 18]. However, most of the experimental studies on such evacuations did not specify the types of disasters owing to the complexity of the environment setting for each disaster, but instead focused on general evacuation behaviors.

In recent years, with the spread of security cameras and smart devices, several video images of evacuations have been accumulated. By analyzing this footage, a new approach has emerged to investigate real-life human evacuation behaviors. This approach led to the discovery of particular evacuation behaviors such as when people prefer a safer place than a place near the door during high intensity tremors, to maintain social attachment during evacuation, to follow the actions of the majority, and to stay in safer and familiar places after an earthquake [8]. The findings of the evacuation behaviors varied among countries [2, 8]. The differences in behaviors between evacuation drills and real-life evacuations [12, 30], and estimations of walking speed during earthquake evacuations [15], were also examined.

In particular, a study of student evacuation behavior analysis in a video by Gu et al. (2016) found that reaction times were linear during evacuation drills but nonlinear in actual evacuation situations. Furthermore, they found that the cumulative curve of the number of evacuees was linear in evacuation drills and nonlinear in actual situations [12].

Although video databases that accumulate such evacuation videos have been created and are being used by researchers [2], many videos only partially record the situation, and few of them can be used for quantitative analysis.
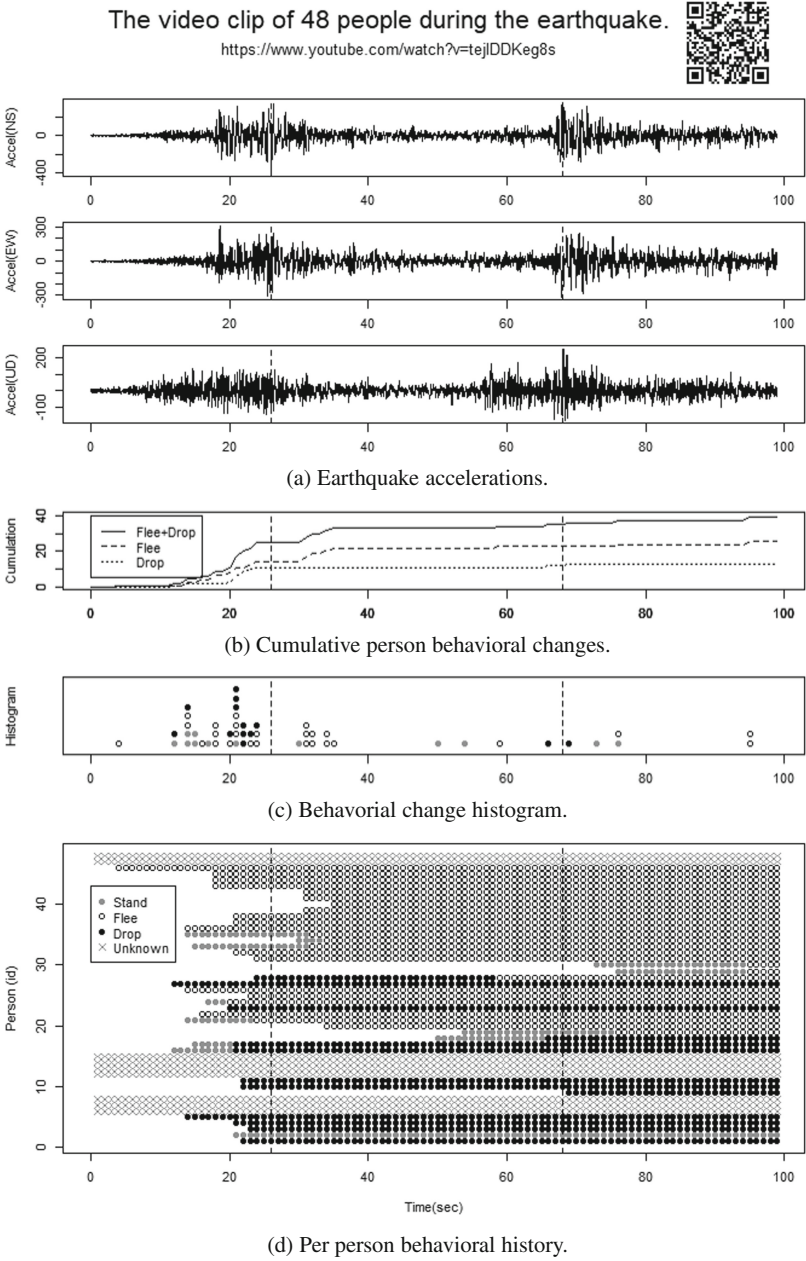
The video clip of 48 people during the earthquake.
https://www.youtube.com/watch?v=tejlDDKeg8s

(a) Earthquake accelerations.

(b) Cumulative person behavioral changes.

(c) Behavorial change histogram.

(d) Per person behavioral history.

Fig. 1. Temporal behavioral changes in 99 s, of 48 people in the video [28].

Most studies have focused on fleeing behaviors during evacuations, and only a few studies have mentioned drop, cover, and hold-on actions [2, 8]. In this study, by analyzing videos captured during the Great East Japan Earthquake, we investigated the

decisions of the evacuees between performing a drop, cover, and hold-on action or fleeing the room.

3 Video Analysis

At 14:46 on March 11, 2011, the Great East Japan Earthquake with a magnitude of 9.0 occurred off the coast of Japan. The video footage in Fig. 1 was taken during an earthquake in a hotel conference room in Miyagino-ku, Sendai City, Miyagi Prefecture. This video records the evacuation behaviors of 48 people during the earthquake. We created quantitative data on the evacuation behaviors of the 48 people by closely tracking each of these behaviors visually. However, the last 40 s were excluded from the analysis owing to a power outage in the video. The following three types of evacuation behavior are recorded in the video:

1. standing and remaining at the current position (Stand),
2. exiting and fleeing from the room (Flee), and
3. hiding under the table, also known as "drop, cover, and hold-on" (Drop)

This data consists of the times when Stand, Flee, and Drop actions were taken for each of the 48 people, and their indoor positions at the time of the earthquake. These data are organized in Fig. 1b–d.

Figure 2 depicts the initial positions of all 48 people when the earthquake started. The room is square-shaped, with only one exit shown in the lower right corner. Initially, all 48 people were sitting at tables in a square, with everyone facing inward.

Figure 1d shows the temporal behavioral changes for each of the 48 people for 99 s after the shaking started. In the chart, the gray, white, and black circles indicate standing, fleeing, and dropping behaviors, respectively, whereas × indicates a behavior that is unidentifiable from the video. For example, the first person to take action (Flee) is No. 46, which shows that it was 4 s after the start of the earthquake. The last person to take action (Stand) was No. 29, indicating that he had been sitting in a chair for 75 s after the start of the earthquake. Figure 1c depicts the number of times that people changed their behaviors. For example, a person changing his/her behavior from sitting to fleeing is indicated by a white circle at the time the behavior changed. Figure 1b shows a cumulative curve of the number of behavioral changes in people. Figure 1c. The dotted, dashed, and solid lines indicate dropping, fleeing, and the sum of both behaviors, respectively. Figure 1a depicts the acceleration generated by the earthquake in the North-South, East-West, and up-down directions[1]. Two vertical dashed lines at 28 and 68 s indicate the two peaks of shaking intensity. As shown in Fig. 1b, in the actual earthquake evacuation, the cumulative curve of the number of people taking part in evacuation behaviors is a convex curve. This is consistent with the results of Gu et al. (2016), in which the cumulative curve in evacuation drills is linear and the cumulative curve in actual evacuations is a convex curve [12].

---

[1] https://www.data.jma.go.jp/svd/eqev/data/kyoshin/jishin/110311_tohokuchiho-taiheiyouoki/index.html
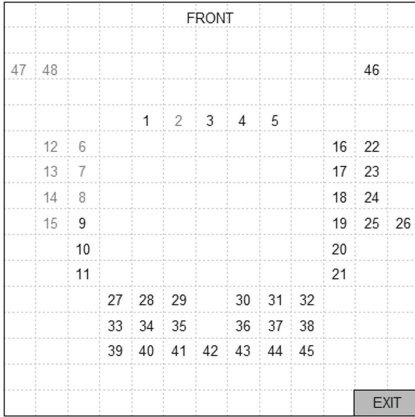(Observation Point: Sendai-shi, Miyagino-ku, Gorin).

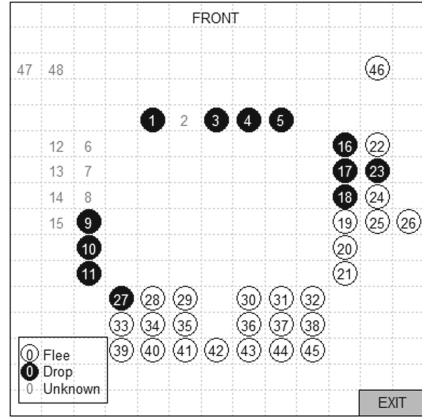**Fig. 2.** Initial location of people in video [28].

Fig. 3. Selection of drop and flee at end of video [28].

Figure 3 shows the final actions taken by 48 people 99 s after the start of the earthquake at their respective initial positions. A white circle with a black number denotes an evacuee who selected a fleeing behavior, and a black circle with a white number denotes an evacuee who selected a dropping behavior. A gray number is an evacuee whose behavior is unknown. In summary, 26 evacuees fled, and 12 evacuees dropped.

Figure 3 illustrates that most people close to the exit decided to flee, whereas those farther from the exit decided to drop, which is an intriguing behavior that had not been previously reported. The boundary between fleeing and dropping crosses the room diagonally, as if people within a certain distance from the exit decided to flee and the others decided to drop, leading to the following hypothesis.

Hypothesis 1. The evacuation decision between fleeing or dropping is based on the distance from the exit.

However, a different hypothesis can be considered for this phenomenon.

Hypothesis 2. The herd behavior among people causes a diagonal spatial pattern even if all individuals randomly choose to flee or drop.

This means that people are consciously making only random choices, but herd behaviors that work between people automatically produce diagonal spatial patterns. Herd behavior is a behavior possessed by many animals including humans and is frequently observed in evacuation situations. Therefore, it is worthwhile to examine this hypothesis.

It is clear that Hypothesis 1 can generate a diagonal spatial pattern. However, this hypothesis requires higher-level cognitive processes such as rules, scenarios, or procedures to estimate the distance to the exit and to judge whether this distance is above a certain threshold. By contrast, Hypothesis 2 requires only lower-level cognitive processes, i.e., herd behaviors, which are typical in many organisms.

The purpose of this study is to show that Hypothesis 2 holds by multiagent simulation using agents that incorporate only random selection and herd behavior. Since actions other than the herd behaviors implemented in the agents are merely random choices, this simulation model implies that simple herd behavior is a sufficient condition for generating the diagonal spatial patterns from which Flee and Drop decisions emerge.

4   Evacuation Decision Model

The evacuation decision model is inspired by the response threshold model in biology [4,5], which represents the division of labor in eusocial organisms, and represents human herd behavior during evacuation [24,26]. The evacuation decision model has been used to analyze cognitive aggregation during evacuation [24] and symmetry breaking in exit choice [26].

In the evacuation decision model, the environment has an objective risk value r, which refers to the severity of the disaster threat. Agent i in the environment has two mental states: $X_i = 0$ and $X_i = 1$. When $X_i = 1$, the agent decides its own action according to its own intention, but when $X_i = 0$, the agent decides its own action depending on the actions of surrounding agents. The former state is called the leader, and the latter state is called the follower. During evacuation, the value of X_i always changes with a certain probability. As a result, agents sometimes act as leaders and sometimes as followers.

The agent has a parameter θ_i, called a response threshold, that determines the degree to which the agent participates in the evacuation. The values of θ_i vary by agent. The probability that an agent will become a leader per unit time is [28]

$$P(X_i = 0 \rightarrow X_i = 1) = \frac{\hat{s_i}^2}{\hat{s_i}^2 + \theta_i^2}, \tag{1}$$

where $\hat{s_i}$ is the local estimation in the stimulus of the environment associated with agent i. This probability depends only on the response threshold θ_i and the environmental stimulus $\hat{s_i}$; however, no individual agent can sense the true value of the environmental stimulus s_i. The value used in the calculation is $\hat{s_i}$, a local estimate of the true environmental stimulus.

The probability that an agent will become a follower per unit time is [28]

$$P(X_i = 1 \rightarrow X_i = 0) = \epsilon, \tag{2}$$

where ϵ is a fixed probability common to all agents. This value is given in the simulation parameters. The estimation of the stimulus of agent i per unit time is given by the following difference equation: [28]

$$s_i(t+1) = max\{s_i(t) + \hat{\delta} - \alpha(1 - R)F,\ 0\ \}, \tag{3}$$

where $\hat{\delta}$ is an increase in the stimulus per unit time [28]

$$\hat{\delta} = \begin{cases} \delta & \text{if } r > 0 \\ 0 & \text{otherwise,} \end{cases} \tag{4}$$

and α is a scale factor of the stimulus. Additionally, R is the risk perception function, which is a function of the objective risk r [28]:

$$R(r) = \frac{1}{1 + exp(-g(r - \mu_i))},$$ (5)

where g is the activation gain determining the shape of the sigmoid function. Additionally, μ_i is the risk perception of agent i, which represents an individual's sensitivity to risk. The evacuation progress function, i.e., the local estimation of the evacuation progress of agent i, is [28]

$$F(n) = \begin{cases} 1 - n/N_{max} & n < N_{max} \\ 0 & \text{otherwise,} \end{cases}$$ (6)

where N is the number of agents in the vicinity that have not yet taken an evacuation action, and N_{max} is the maximum number of agents in the vicinity. In other words, the agents judge that the overall evacuation has not yet progressed if the ratio of agents in the vicinity who have not taken evacuation action is large, or that progress has been made if the ratio is small.

5 Earthquake Evacuation Simulation

The purpose of this study is to show that Hypothesis 2 in Sect. 3 can reproduce the convex curve of the cumulative number of evacuees in Fig. 1b and the diagonal spatial pattern in Fig. 3 using multiagent simulations. This section describes the details of this simulation. This simulation setting represents a situation similar to the video in Fig. 1, but it is not exactly the same. The simulation model was implemented using NetLogo 6.0.2 [29].

5.1 Configuration

A square room of 40×40 units with the lower right as the origin is the environment for this simulation. This room has one exit at the bottom right. Initially, 500 agents $A = \{a_1, a_2, \ldots, a_{500}\}$ are randomly distributed in the region from 3 to 38 units for the X and Y coordinates. Assuming a simulation time of $t = 1, \ldots, T$, an agent $a_i \in A$ has coordinates $x_i(t), y_i(t) \in \mathbb{R}$, a local estimation of stimulus $s_i(t) \in \mathbb{R}$, mental state $X_i(t) \in \{1, 0\}$, and an action $\pi_i(t) \in \{undecided, flee, drop\}$, where *undecided* indicates that the agent has not yet determined an action, *flee* indicates that the agent has decided to flee, and *drop* indicates that the agent has decided to drop. In this simulation, both Flee and Drop are evacuation behaviors; therefore, the value of n in Eq. 6 is $n = |\{a_j \, in V_i \mid \pi_j(t) = undecided\}|$. Furthermore, an agent has two parameters: response threshold θ_i and risk sensitivity μ_i. Let $x_i(1), y_i(1) \sim U(3, 38)$, $s_i(1) = 0$, $X_i(1) = 0$, $\pi_i(1) = undecided$, $\theta_i \sim U(0, 100)$, and $\mu_i \sim U(0, 100)$ be the initial values of the simulation, with the simulation terminated at $T = 270$.

The vicinity of a_i is defined as $V_i = \{a_j \in A \mid \nu(a_j, a_i)\}$, where $\nu : A^2 \to \{true, false\}$, and ν refers to a range of five units $120°$ toward the direction of motion of a_i.

Algorithm 1. Leader's action (Random Selection) [28].

> **if** $\pi_i(t) = undecided$ **then**
> $\tau \sim U(0,1)$
>   **if** $\tau \leq 0.5$ **then**
> $\pi_i(t) \Leftarrow drop$
>   **else**
> $\pi_i(t) \Leftarrow flee$
>   **end if**
> **end if**
> **if** $\pi_i(t) = flee$ **then**
>   Solve Problem 1 and determine $\Delta x, \Delta y$
> $x_i(t) \Leftarrow x_i(t) + \Delta x; \;\; y_i(t) \Leftarrow y_i(t) + \Delta y$
> **end if**

Algorithm 2. Follower's action (Herd Behavior) [28].

> $n_d \Leftarrow |\{a_j \in V_i \mid \pi_j(t) = drop\}|$
> $n_e \Leftarrow |\{a_j \in V_i \mid \pi_j(t) = flee\}|$
> $n_u \Leftarrow |\{a_j \in V_i \mid \pi_j(t) = undecided\}|$
> **if** $n_d > n_e$ **and** $n_d > n_u$ **then**
> $\pi_i(t) \Leftarrow drop$
> **else if** $n_e > n_d$ **and** $n_e > n_u$ **then**
> $\pi_i(t) \Leftarrow flee$
> **end if**
> **if** $\pi_i(t) = flee$ **then**
>   Solve Problem 1 and determine $\Delta x, \Delta y$
> $x_i(t) \Leftarrow x_i(t) + \Delta x; \;\; y_i(t) \Leftarrow y_i(t) + \Delta y$
> **end if**

At each time step, an agent with $\pi_i(t) = flee$ moves toward the exit $(G_x, \; G_y)$ by $\Delta x, \Delta y$, as determined by solving Problem 1 [28].

Problem 1

$$min \; (x_i(t) + \Delta x - G_x)^2 + (y_i(t) + \Delta y - G_y)^2 \tag{7}$$
$$s.t. \qquad \Delta x^2 + \Delta y^2 = 1 \tag{8}$$

An agent with $\pi_i(t) \neq flee$ remains at the same position, i.e., $\Delta x = 0$ and $\Delta y = 0$.

The procedure for the entire simulation is shown in Algorithm 3. Agent a_i executes Algorithm 1 when $X_i = 1$ and Algorithm 2 when $X_i = 0$. Agents decide their behaviors based on their own intentions only when Algorithm 1 is executed; this is a random selection.

The room has an objective risk that starts at $r(1) = 0$ and increases by 1 for each time step up to the maximum value of $r(t) = 100$. The local estimation of the stimulus of a_i starts at $s_i(1) = 0$ and is incremented by δ at each time step as $F \approx 0$ during the initial stages of the simulation. Thus, $P(X_i = 0 \rightarrow X_i = 1)$ gradually increases depending on θ_i, resulting in the emergence of leader agents. Subsequently, followers appear, and herding spreads among the agents.

Finally, the overall simulation procedure is shown in Algorithm 3. The following parameters were used: $\alpha = 1.2$, $\delta = 0.5$, $\epsilon = 0.2$, $g = 1.0$, and $N_{max} = 10$.

Algorithm 3. Simulation.

Initialization
for $t = 1$ to T **do**
   $r \Leftarrow min\{r + 1, \ 100\}$
   for all $a_i \in A$ **do**
      Calculate R {Equation 5}
      Calculate F {Equation 6}
      Calculate s_i {Equation 3}
      $\tau \sim U(0, 1)$
      if $X_i = 1 \wedge \tau < P(X_i = 1 \rightarrow X_i = 0)$ **then**
         $X_i \Leftarrow 0$
         Execute Algorithm 2 {Follower's action (Herd Behavior)}
      else if $X_i = 0 \wedge \tau < P(X_i = 0 \rightarrow X_i = 1)$ **then**
         $X_i \Leftarrow 1$
         Execute Algorithm 1 {Leader's action (Random Selection)}
      end if
      if $(x_i(t) - G_x)^2 + (y_i(t) - G_y)^2 < 1$ **then**
         $A \Leftarrow A \setminus a_i$ {Remove a_i from the environment if the exit has been reached.}
      end if
   end for
end for

5.2   Result 1

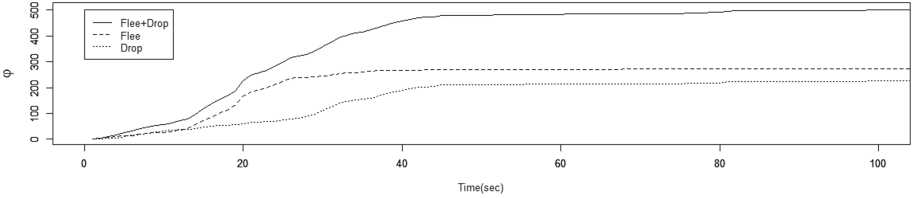In this section, the results of the simulation described in Sect. 5.1 are presented.

Fig. 4. Cumulative number of evacuees over simulation time [28].

Figure 4 shows the cumulative curves of the evacuees who conducted evacuation actions per simulation time. The solid line in the chart is obtained through the function $\varphi(t)$ [28]:

$$\varphi(t) = \varphi(t - 1) + \sum_{a_i \in A} \gamma_i(t), \qquad (9)$$

where [28]

$$\gamma_i(t) = \begin{cases} 1 & t = min\{z \mid \pi_i(z) \neq undecided\} \\ 0 & \text{otherwise,} \end{cases} \qquad (10)$$
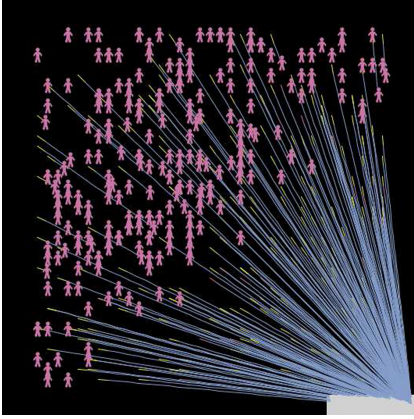
Fig. 5. Distribution of the remaining agents in the room at the end of the simulation. Straight lines towards the exit show the trajectories of fleeing agents.
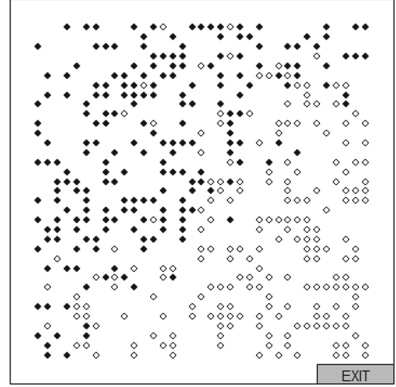

Fig. 6. Initial locations and decisions between fleeing and dropping. Black circles refer to $\pi_i(T) = drop$, and white circles refer to $\pi_i(T) = flee$.

and $\varphi(0) = 0$. The function $\varphi(t)$ is the time change of the cumulative curve of the evacuees who chose Flee or Drop, and is convex upward as in Fig. 1b. This is consistent with the results of Gu et al. (2016) [12].

Figure 5 shows the coordinates $x_i(T), y_i(T)$ of remaining agents in the room at $t = T$. Straight lines to the exit are the trajectories of the agent who chose Flee. There are 249 agents left in the room, all of whom have chosen Drop. All of these agents remain far from the exit, forming a diagonal spatial pattern similar to Fig. 3.

If we divide the room into two spaces with a diagonal line $y = x$ and let the number of agents in the upper-left space be $N_u = |\{a_i \mid y_i(T) \geq x_i(T)\}|$ and the lower-right space be $N_l = |\{a_i \mid y_i(T) < x_i(T)\}|$, we have $N_u = 221$ and $N_l = 28$, with a difference of $N_d = N_u - N_l = 193$.

Here, we adopted entropy to evaluate the simulation results quantitatively [6]. Figure 6 shows the action of each agent at the end of the simulation at their initial location at $t = 1$. The black and white circles represent $\pi_i(T) = drop$ and $\pi_i(T) = flee$, respectively. As shown in Fig. 6, with a few exceptions, most agents initially located in the upper-left space decided to drop, and those in the lower-right space decided to flee. To evaluate whether the decision between fleeing and dropping is divided by the diagonal line $y = x$, entropy H is introduced as follows [28]:

$$H = -r_g \, log_2(r_g) - r_b \, log_2(r_b), \tag{11}$$

where [28]

$$r_g = L_g/(L_g + L_b) \tag{12}$$
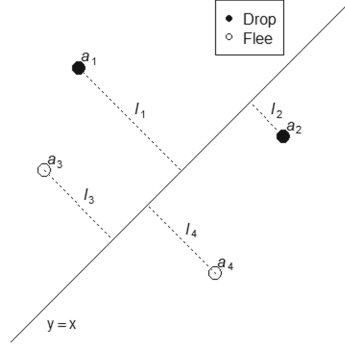$$r_b = L_b/(L_g + L_b), \tag{13}$$

Fig. 7. Calculations of L_g and L_b. In this case, $L_g = l_1 + l_4$ and $L_b = l_2 + l_3$ [28].

and [28]

$$L_g = \sum_{\{a_i | y_i(1) \geq x_i(1) \wedge \pi_i(T) = drop\}} l_i + \sum_{\{a_j | y_j(1) < x_j(1) \wedge \pi_j(T) = flee\}} l_j \qquad (14)$$

$$L_b = \sum_{\{a_i | y_i(1) \leq x_i(1) \wedge \pi_i(T) = drop\}} l_i + \sum_{\{a_j | y_j(1) > x_j(1) \wedge \pi_j(T) = flee\}} l_j, \qquad (15)$$

where [28]

$$l_i = \sqrt{2 \left(\frac{x_i(1) - y_i(1)}{2} \right)^2} \qquad (16)$$

and l_j is the minimum distance between the initial position of a_i and the diagonal $y = x$. Additionally, L_g is the sum l_i of the shortest distances to the diagonal from the initial position of a_i in the upper-left space with $\pi_i(T) = drop$ and an agent in the lower-right space with $\pi_i(T) = flee$. Conversely, L_b is the sum of l_i of the shortest distance to the diagonal from the initial position of agent a_i in the upper-left space with $\pi_i(T) = flee$ and an agent in the lower-right space with $\pi_i(T) = drop$. For example, in the case of Fig. 7, $L_g = l_1 + l_4$ and $L_b = l_2 + l_3$.

With a smaller H, fleeing and dropping behaviors are delineated by the $y = x$ diagonal, whereas the behavior becomes intermingled if H is close to 1.0. The entropy shown in Fig. 6 is $H = 0.18$.

We used the distance from $y = x$ instead of the number of agents in the calculation of entropy because the positions of the remaining agents are also important when evaluating the diagonal spatial pattern.

5.3   Result 2

In order to generalize the results in Sect. 5.2, 500 simulations were conducted, and the results of these simulations are presented in this section. The time evolution of the cumulative number of evacuees in the 500 simulations of $\Phi(t) = \overline{\varphi(t)}$ is shown in Fig. 8. This curve is convex upward and smoother than that of Fig. 4.
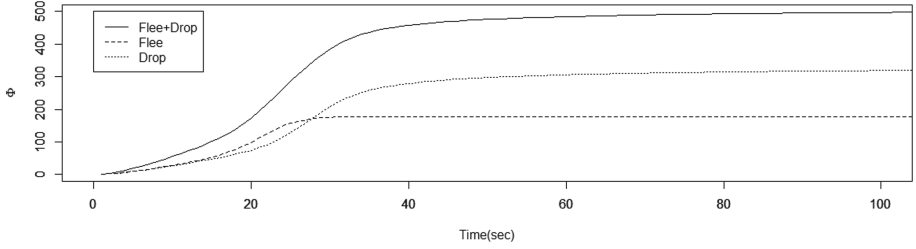
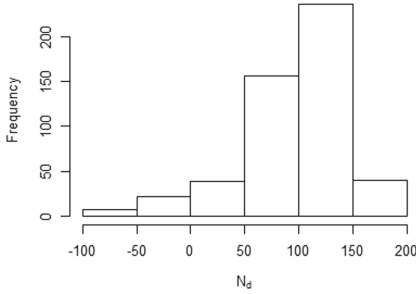**Fig. 8.** Mean values of $\varphi(t)$ and $\Phi(t)$, for 500 simulations.
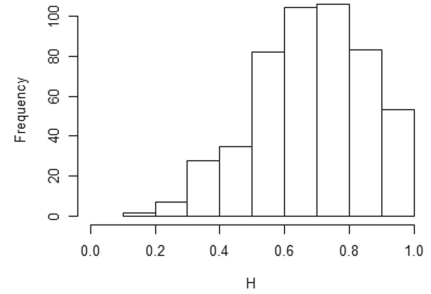

Fig. 9. Histogram of N_d.

Fig. 10. Histogram of H.

A histogram of the difference N_d in the number of agents in the space divided by the diagonal line $y = x$, as shown in Fig. 9, and a histogram of the entropy H of decision-making at the time of evacuation are shown in Fig. 10. The mean, standard deviation (σ), and minimum and maximum values of N_d and H are summarized in Table 1.

Table 1. Statistics of N_d and H for 500 simulations.

	min	mean	σ	max
N_d	−89.0	96.83	48.04	192
H	0.15	0.68	0.18	1.00

Figure 11 is the kernel density distribution of the coordinates $x_i(T)$, $y_i(T)$ of the agents remaining in the room at $t = T$. The figure shows a higher kernel density at a farther position and a lower kernel density at a closer position, illustrating a high correlation between the distance from the exit and the agents remaining in the room at the end of the simulation. This shows that simple herd behavior is sufficient to reproduce a diagonal spatial pattern recorded in the video clip during the Great East Japan Earthquake.
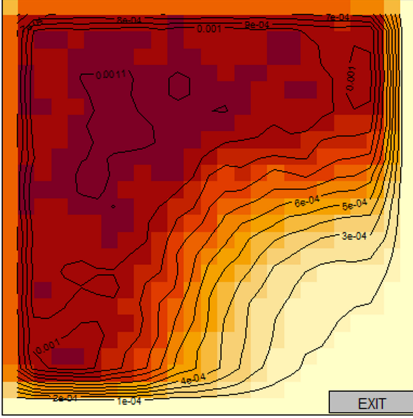
Fig. 11. Kernel density of $x_i(T)$ and $y_i(T)$ throughout room. Dark areas represent high density, and light areas represent low density.
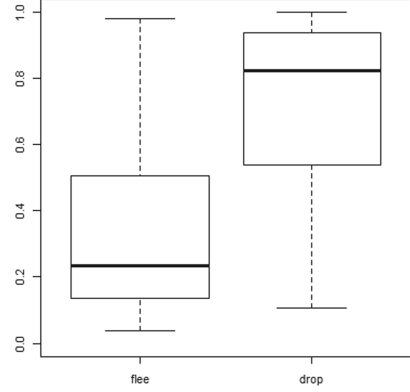
Fig. 12. Logit model discriminating between dropping and fleeing [28].

6   Analysis

We conducted three analyses to examine the results of the simulations. First, we conducted a logistic regression analysis to explore the primal factor that gives rise to the diagonal spatial pattern. Second, a graph centrality analysis was applied to uncover the influence dynamics among agents during the evacuation. Finally, a sensitivity analysis was conducted to investigate the robustness and parameter sensitivities of the results.

6.1   Logistic Analysis

In a previous study [28], we conducted a logistic regression analysis to investigate the effect of each parameter of the agent on the final decision $\pi_i(T)$ by assuming $drop = 1$ and $flee = 0$. The parameters are response threshold θ_i, risk sensitivity μ_i, and distance from the exit [28]

$$L_i = \sqrt{(x_i(1) - G_x)^2 + (y_i(1) - G_y)^2}. \tag{17}$$

A total of 200 and 500 training and test samples, respectively, were randomly selected from 75,000 samples (500 agents $\times$ 150 simulations in [28]). Large amounts of training data reduce both the p-value and the reliability of the analysis; therefore, we

Table 2. Results of logistic analysis. Coefficients and P-values [28].

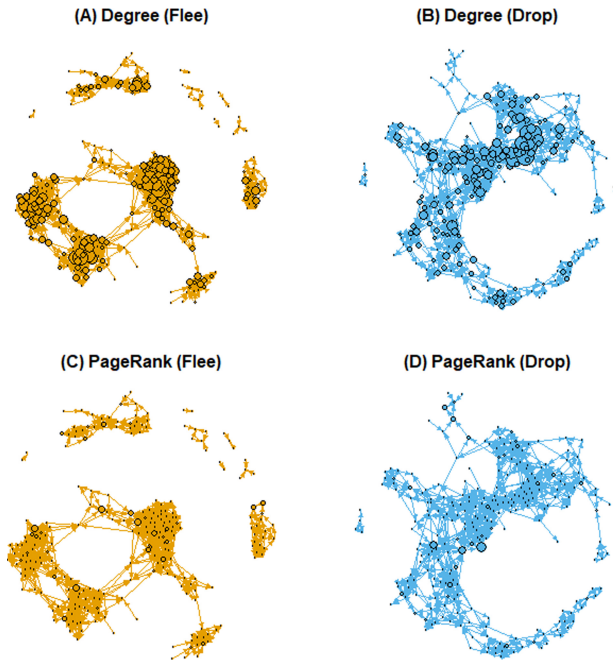|	Intercept	L_i	θ_i	μ_i
coeff	-3.4486	0.0033	0.0115	0.0055
P-values	0.0	0.0	0.0796	0.3532

Fig. 13. Influence graphs with centralities. From left, size of nodes shows degree of fleeing, degree of dropping, PageRank of fleeing, and PageRank of dropping agents.

set the number of training data to 200 samples. The results of the logistic regression analysis in terms of the coefficients and p-values are shown in Table 2. From Table 2, the primary factor in the drop or flee decision is the distance between the agent and the exit ($p < 0.01$). This implies that the response threshold θ_i may have certain effects on the decision ($p < 0.1$), whereas the risk sensitivity μ_i may not have any effect ($p > 1$).

We attempted to discriminate 500 test data by using a logit model created by the logistic regression analysis. The results are shown in Fig. 12. The figure shows that the logit model is capable of discriminating between Drop and Flee for unknown data.

6.2 Graph Centrality Analysis

In this section, we focus on the results presented in Sect. 5.2 and investigate how agents influence each other during the evacuation processes using social network analysis techniques. Influences among agents are dynamic and complex because an agent imitates the behaviors of nearby agents that vary from time to time owing to a herd behavior. The decision of one agent affects the behaviors of the other agents that happen to be within the vicinity of the agent, and these behaviors may influence the first agent later. This interconnected system of influence among the evacuees forms a complex network.

Figure 13 shows directed graphs of the influences among agents. A node represents an agent, and an arrow connecting two agents represents the influence of herd behaviors between them; the root node affects the arrowhead node. The size of the node represents
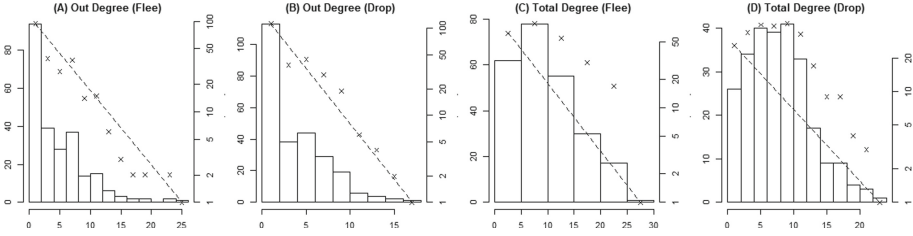
Fig. 14. Graph Centrality Histograms: (A) out-degrees of fleeing agents, (B) out-degrees of dropping agents, (C) total degrees of fleeing agents, and (D) total degrees of dropping agents. Additionally, ×s show value of histograms on logarithmic scale.

the centrality of that node in the graph. In Fig. 13, graph (A)—the degree of centrality of a fleeing agent, graph (B)—a dropping agent, graph (C)—the PageRank centrality of a fleeing agent, and graph (D)—a dropping agent. In the first and second graphs (i.e., graphs A and B in Fig. 13), as we were interested in studying attributes of affecting agents, we limited the edges towards the leaving directions to calculate the degree of centralities of the nodes (out-degrees).

Figure 14 shows the frequencies of the node degrees of the graphs given in Fig. 13. Histograms of the node degrees of the graphs in Fig. 13 are presented in Fig. 14 (the left axes), and the values of these histograms (×s in the charts in Fig. 14) are also plotted on the logarithmic scale (the right axes) over these histograms. The first and second charts in Fig. 14 show histograms of out-degrees, and the third and fourth charts show histograms of the total degrees. In the first and second charts (A and B in Fig. 14), a few nodes have high out-degrees, whereas most of the nodes have low out-degrees; in addition, ×s are on the straight dashed line yielding a scale-freeness of the graphs. However, this does not hold for the third and fourth charts (C and D in Fig. 14), and the scale-freeness is not observed for the total-degree graphs.

In the graphs of the fleeing agents (A and C in Fig. 13), we can see a small number of clusters connected by a few agents, meaning that many agents egress in the form of groups. By contrast, in the graphs of the dropping agents (B and D in Fig. 13), almost all agents are connected and form one large cluster, meaning that the influences of the dropping behaviors propagate over all dropping agents and interconnect them.

In comparison, the degree of centrality graphs (A and B in Fig. 13) have more nodes with high centralities than PageRank centrality graphs (C and D in Fig. 13). Despite scale-freeness, in the degree of centrality graphs, many agents still affect each other. In other words, there is no evidence indicating that more agents are affected by a few specific agents.

PageRank centrality, which is an eigenvector with the highest eigenvalues of the transition matrix representing the influence graph, illustrates important nodes that are affected by many agents and may affect many others. The PageRank centrality graphs in Fig. 13 show that a few nodes are more important than the other nodes, although the sizes of these nodes are relatively small. This implies that the effects of these important nodes might be insignificant. To verify this, we eliminated the top five agents that had the highest PageRank from the original setting presented in Sect. 5.2 and conducted a
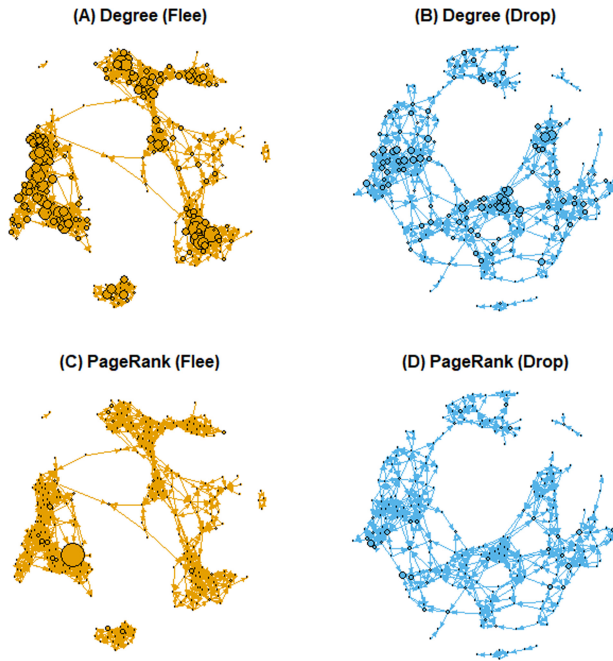
Fig. 15. Influence graphs with centralities when removing top five agents with highest PageRank.

new simulation. Figure 15 shows centrality graphs of the simulation results. Comparing Figs. 13 and 15, the main features of these graphs show only slight changes even though some nodes with a high PageRank were eliminated, indicating that these features presented in the analysis cannot be altered by changing the behaviors of a small number of agents.

6.3 Sensitivity Analysis

Thus far, we have conducted simulations with a vicinity setting of five units for the distance and 120° toward the heading direction of an agent. During a herd behavior, an agent selects the behavior adopted by the highest number of agents within his/her vicinity (Algorithm 2). Thus, the definition of the vicinity of an agent is crucial; subsequently, the final results of the simulations depend on this definition, and the agent considers the decisions of the other agents within this range to make his/her own decision. Therefore, we conducted simulations by varying the definition of the vicinity of the agents to examine the sensitivity of the defined vicinity on the results.

Figure 16 shows the results of the sensitivity analysis. The distance was varied from 0 to 20 units (rows), and the angle was varied from 20 to 360° (columns). Each cell in the figure refers to the result of 100 simulations for the given settings; in addition, dark areas represent the high densities of the dropping agents remaining at the end of the simulation, and light areas represent low densities.
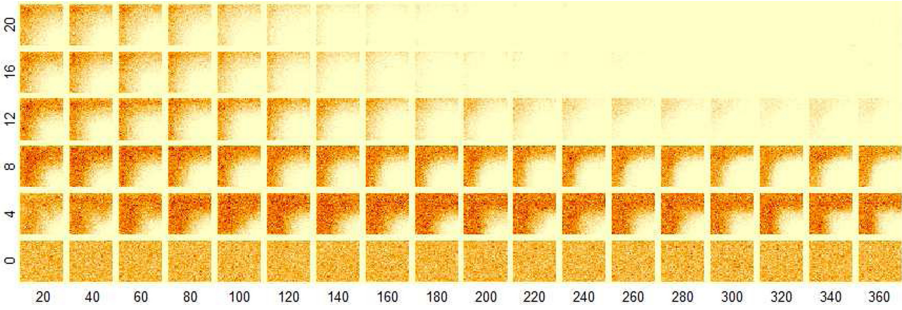
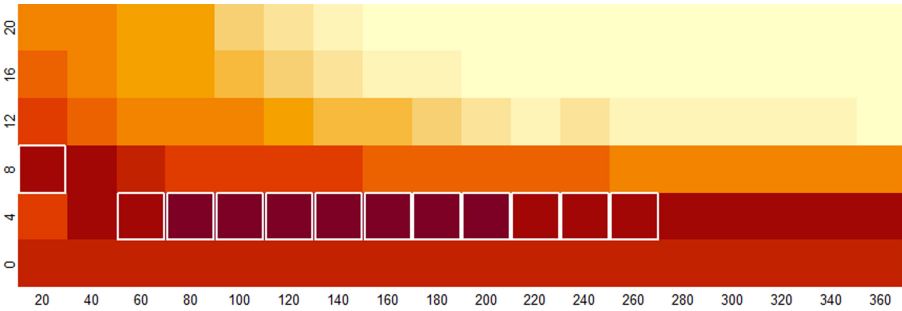**Fig. 16.** Final positions of remaining agents with varying distances and angles of agent vicinities.

Fig. 17. Total number of remaining agents with varying distances and angles of agent vicinities.

In Fig. 16, the results similar to Fig. 11 can be observed within a broad range in the figure, showing that these results are insensitive to the vicinity definitions. However, a closer look raises a few more interesting insights. Notice that most cells in the upper-right areas of the figure have light colors, which means that a small number of agents remained at the end of the simulations. This area represents vicinities with long distances and wide angles, referring to extensive vicinities. Figure 17 shows a heat map of the mean number of remaining agents (dropping agents) at the end of the simulations; light colors show low populations, and dark colors show high populations. This figure also indicates low populations in the upper-right areas. These two figures also depict high populations in the lower-left areas; however, the highest population area is not located at the lowest and leftmost corner in Fig. 17. The white square frames in Fig. 17 indicate that the mean number of remaining agents is higher than 300. The lowest row refers to settings with a distance of zero, i.e., agents with no vicinity, yielding simulations without herd behaviors. Therefore, the only behavior the agents can take is a random choice between fleeing and dropping. The lowest rows in Fig. 16 show that the remaining agents are distributed throughout the area evenly. In these cells, the mean number of remaining agents is 250 because each agent merely makes an independent random choice. The observation in this section reveals that broad vicinities propagate fleeing behaviors toward a widespread range of the environment, and limited
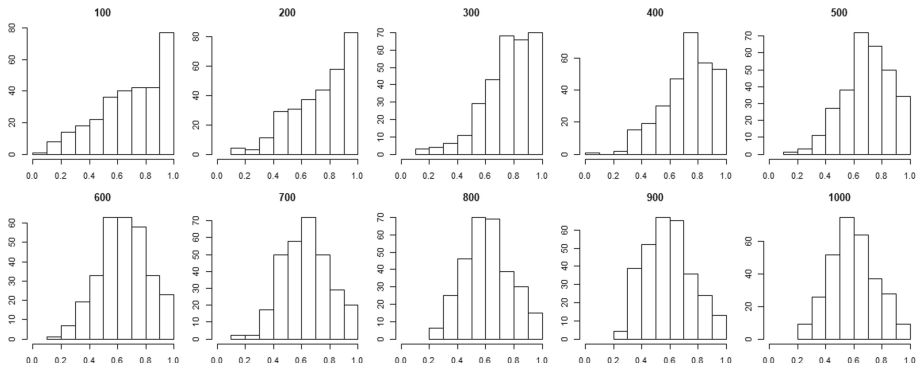
Fig. 18. Histograms of the number of remaining agents with varying populations of agents.
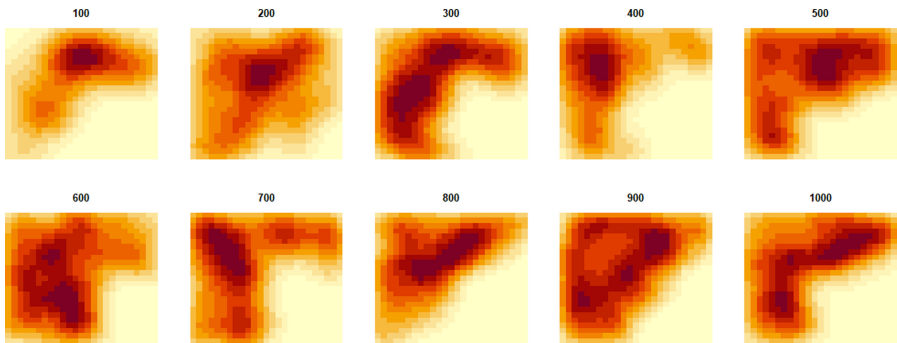

Fig. 19. Final positions of remaining agents with varying populations of agents.

vicinities propagate dropping behaviors. However, if the vicinities are too small, then agent behaviors approach a simple random choice because the effect of the herd behaviors becomes negligible.

Population density is another important factor affecting the simulation results because the number of agents within the vicinity depends on the density of the agents. We conducted experiments by varying the number of agents in the environment from 100 to 1000; each experiment consisted of 300 simulations. Figure 18 shows a histogram of H for each experiment. The values of H are distributed over a broad range of domains; however, the figure shows that population densities affect the peaks of the distributions. The peak is close to 1 when the population is low, whereas it becomes close to 0.5 if the population is high.

Figure 19 depicts heat maps of the final positions of the remaining agents for each experiment; the ranges with dark colors represent the areas with high frequencies of remaining agents, whereas light colors represent the areas with low frequencies. In all diagrams in Fig. 19, the lower-right areas in each heat map have light colors, leading to low densities of the remaining agents, which are in good agreement with Fig. 11. The results of the sensitivity analysis revealed that the unusual evacuation behaviors

captured in the video clip are unaffected by the population density of the agents (Fig. 19), and a higher population density will bring about higher frequencies of this phenomenon (Fig. 18).

7   Discussion

Our simulation results in Figs. 5 and 6 show that the decision between dropping and fleeing is determined by the distance from the exit. However, Figs. 9 and 10 indicate that the results from the simulation vary, i.e., the results described in Sect. 5.2 are not always obtained. Contrary to our expectations, some simulations showed $N_d = -89$, signifying that more agents remained in the area closer to the exit, whereas other simulations resulted in $H \approx 1.00$, implying a combination of dropping and fleeing behaviors.

Although we concede that exceptional cases like these do occur, the evacuation decision model is clearly able to produce results similar to our findings from the video analysis of the Great East Japan Earthquake, albeit at a slightly lower frequency. The kernel density of the results in Fig. 11 agrees well with the statement above. Furthermore, the results of the logistic regression analysis revealed that the primary factor in deciding between dropping and fleeing for individual agents was the distance between their initial location and the exit. Nonetheless, Hypothesis 2 suggests that each individual does not have to consider this distance to determine his/her behavior; rather, a simple herd behavior is sufficient to produce a diagonal spatial pattern.

The analysis described in Sect. 6.2 illustrates that the influences among the agents form a complex scale-free network. The experiment removing the top-five highest PageRank agents resulted in another complex network, implying that the nature of the network is unaltered by modifying a small number of agents. Guiding the crowd toward safer evacuations behaviors is useful and desirable. The centrality analysis conducted in our studies suggests that controlling a small number of evacuees is insufficient to control the behaviors of the entire crowd. The sensitivity analysis described in Sect. 6.3 indicates that the diagonal spatial pattern captured in the video clip of the Great East Japan Earthquake can be reproduced within a broad range of population and vicinity parameters. The diagonal spatial pattern is robust and insensitive to the model parameters.

As the most remarkable aspect of this analysis, the results were produced by agents who have no higher-level cognitive processes. The agents in our model performed only either imitations or random selections, both of which are unintelligent behaviors. Neither distance estimations nor thresholds are necessary to reproduce the behaviors in the video. From the discussion thus far, we conclude that Hypothesis 2 holds.

The fact that Figs. 4 and 8 are consistent with Fig. 1b, and that the cumulative curve of the evacuees shows convex and real evacuation situations [12], provides additional support that our simulations using the evacuation decision model can yield realistic results.

Hypothesis 2 and the results of the analyses above indicate that

1. the primal factor of the phenomenon is the distance from the exit,
2. the scale-freeness of the network is robust, and
3. the phenomenon is insensitive to the model parameters.

This may suggest that the diagonal spatial pattern captured in the video clip is induced more by physical factors than by intentional cognitive factors of the agents.

We do not deny Hypothesis 1; rather, we consider it natural for people close to the exit to select a fleeing action intentionally. In reality, we believe that both Hypothesis 1 and Hypothesis 2 hold simultaneously. A real evacuation process is a complex combination of higher-level cognitive processes such as decision-making and lower-level cognitive processes such as herd behavior. Some researchers also pointed out the importance of an individual's emotional responses during crowd evacuation processes [16].

This study demonstrated that an evacuation decision model can reproduce the real human evacuation behaviors that were recorded in a video of the Great East Japan Earthquake and can be used to analyze human herd behaviors during an earthquake. Tsurushima [26,27] demonstrated that a simple herd behavior can reproduce symmetry breaking in exit selection when using the evacuation decision model. Furthermore, the analysis presented herein revealed the significance of herd behavior in collective evacuations. Hence, the evacuation decision model is advantageous for a quantitative analysis of the effects of herd behavior in human evacuations.

Finally, some potential methodological weaknesses should be considered. The video clip analyzed in this study is the only instance in which we can find the specific evacuation behavior discussed in this paper. We do not know the universality of these behaviors under other evacuation scenarios. There is also a possibility of errors occurring in the video analysis phase because this process was controlled manually. The simulation was not configured identically with the actual events captured in the video, for example, the number or initial layout of the agents. It would be interesting to experiment with a more realistic design, and a comparison of these two studies may bring about some new findings of crowd evacuations. However, such experiments are reserved for a future study.

8 Conclusion

By analyzing a video captured during the Great East Japan Earthquake, we discovered that the decision between dropping and fleeing was influenced by the distance to the exit, a finding that was not previously reported. We reproduced this finding, which is the diagonal spatial pattern of the remaining evacuees, using an evacuation decision model, and revealed that simple herd behaviors are sufficient to reproduce this phenomenon. Analyses of the simulation results show that these results are robust and insensitive to the model parameters.

References

1. Altshuler, E., Ramos, O., Nuñez, Y., Fernańdez, J., Batista-Leyva, A.J., Noda, C.: Symmetry breaking in escaping ants. Am. Nat. **166**(6), 643–649 (2005)

2. Bernardini, G., Lovreglio, R., Quagliarini, E.: Proposing behavior-oriented strategies for earthquake emergency evacuation: a behavioral data analysis from new Zealand, Italy and Japan. Saf. Sci. **116**, 295–309 (2019)

3. Bode, N., Holl, S., Mehner, W., Seyfried, A.: Disentangling the impact of social groups on response times and movement dynamics in evacuations. PloS One **10**, e0121227 (2015)

4. Bonabeau, E., Theraulaz, G., Deneubourg, J.L.: Quantitative study of the fixed threshold model for the regulation of division of labour in insect societies. Proc. R. Soc. B **263**(1376), 1565–1569 (1996)

5. Bonabeau, E., Theraulaz, G., Deneubourg, J.L.: Fixed response thresholds and the regulation of division of labor in insect societies. Bull. Math. Biol. **60**, 753–807 (1998)

6. Crociani, L., Vizzari, G., Yanagisawa, D., Nishinari, K., Bandini, S.: Route choice in pedestrian simulation: design and evaluation of a model based on empirical observations. Intelligenza Artificiale **10**, 163–182 (2016)

7. Cutter, S., Barnes, K.: Evacuation behavior and three mile Island. Disasters **6**(2), 116–124 (1982)

8. D'Orazio, M., Spalazzi, L., Quagliarini, E., Bernardini, G.: Agent-based model for earthquake pedestrians' evacuation in urban outdoor scenarios: behavioural patterns definition and evacuation paths choice. Saf. Sci. **62**, 450–465 (2014)

9. Drury, J., Brown, R., González, R., Miranda, D.: Emergent social identity and observing social support predict social support provided by survivors in a disaster: solidarity in the 2010 Chile earthquake. Eur. J. Soc. Psychol. **46**(2), 209–223 (2015)

10. Elliott, D., Smith, D.: Football stadia disasters in the United Kingdom: learning from tragedy? Ind. Environ. Crisis Q. **7**(3), 205–229 (1993)

11. Garcimartín, A., Zuriguel, I., Pastor, J., Martín-Gómez, C., Parisi, D.: Experimental evidence of the "faster is slower" effect. In: Transportation Research Procedia: The Conference on Pedestrian and Evacuation Dynamics (PED 2014), Delft, The Netherlands, vol. 2, pp. 760–767, 22–24 October 2014

12. Gu, Z., Liu, Z., Shiwakoti, N., Yang, M.: Video-based analysis of school students' emergency evacuation behavior in earthquakes. Int. J. Disaster Risk Reduction **18**, 1–11 (2016)

13. Haghani, M., Sarvi, M.: Following the crowd or avoiding it? empirical investigation of imitative behaviour in emergency escape of human crowds. Anim. Behav. **124**, 47–56 (2017)

14. Haghani, M., Sarvi, M.: 'Herding' in direction choice-making during collective escape of crowds: how likely is it and what moderates it? Saf. Sci. **115**, 362–375 (2019)

15. Hori, M.: Introduction to Computational Earthquake Engineering, 3rd edn. World Scientific (Europe), London (2018)

16. Kefalas, P., Sakellariou, I.: The invalidity of validating emotional multi-agent systems simulations. In: Proceedings of the 8th Balkan Conference in Informatics. BCI 2017, pp. 8:1–8:8. ACM, New York, NY, USA (2017)

17. Kimura, R., Hayashi, H., Tatsuki, S., Tamura, K.: Behavioural and psychological reconstruction process of victims in the 2004 mid-niigata prefecture earthquake. In: Proceedings of the 8th US National Conference on Earthquake Engineering, pp. 1–9 (2006)

18. Lovreglio, R., Borri, D., dell'Olio, L., Ibeas, A.: A discrete choice model based on random utilities for exit choice in emergency evacuations. Saf. Sci. **62**, 418–426 (2014)

19. Mas, E., Suppasri, A., Imamura, F., Koshimura, S.: Agent-based simulation of the 2011 great east japan earthquake/tsunami evacuation: an integrated model of tsunami inundation and evacuation. J. Nat. Disaster Sci. **34**(1), 41–57 (2012)

20. Morita, T., Tsukada, S., Yuzawa, A.: Analysis of evacuation behaviors in different areas before and after the great east Japan earthquake. In: Fifth International Conference on Geotechnique, Construction Materials and Environment (2015)

21. Saloma, C., Perez, G.J., Tapang, G., Lim, M., Palmes-Saloma, C.: Self-organized queuing and scale-free behavior in real escape panic. PNAS **100**(21), 11947–11952 (2003)

22. Schmidt, S., Galea, E. (eds.): Behaviour - Security - Cluture (BeSeCu): Human behaviour in Emergencies and Disasters: A Cross-cultural Investigation. Pabst Science Publishers, Lengerich (2013)
23. Shiwakoti, N., Sarvi, M.: Understanding pedestrian crowd panic: a review on model organisms approach. J. Transp. Geogr. **26**, 12–17 (2013)
24. Tsurushima, A.: Modeling herd behavior caused by evacuation decision making using response threshold. In: Pre-proceedings of the 19th International Workshop on Multi-Agent-Based Simulation (MABS2018) - A FAIM workshop. Stockholm, Sweden (2018)
25. Tsurushima, A.: Modeling herd behavior caused by evacuation decision making using response threshold. In: Davidsson, P., Verhagen, H. (eds.) MABS 2018. LNCS (LNAI), vol. 11463, pp. 138–152. Springer, Cham (2019). https://doi.org/10.1007/978-3-030-22270-3_11
26. Tsurushima, A.: Reproducing symmetry breaking in exit choice under emergency evacuation situation using response threshold model. In: Proceedings of the 11th International Conference on Agents and Artificial Intelligence. ICAART, vol. 1, pp. 31–41. INSTICC, SciTePress (2019)
27. Tsurushima, A.: Symmetry breaking in evacuation exit choice: impacts of cognitive bias and physical factor on evacuation decision. In: van den Herik, J., Rocha, A.P., Steels, L. (eds.) ICAART 2019. LNCS (LNAI), vol. 11978, pp. 293–316. Springer, Cham (2019). https://doi.org/10.1007/978-3-030-37494-5_15
28. Tsurushima, A.: Validation of evacuation decision model: an attempt to reproduce human evacuation behaviors during the great east Japan earthquake. In: Proceedings of the 12th International Conference on Agents and Artificial Intelligence. ICAART, vol. 1, pp. 17–27. INSTICC, SciTePress (2020)
29. Wilensky, U.: NetLogo, Center for Connected Learning and Computer-Based Modeling, Northwestern University, Evanston, IL (1999)
30. Yang, X., Wu, Z., Li, Y.: Difference between real-life escape panic and mimic exercises in simulated situation with implications to the statistical physics models of emergency evacuation: The 2008 Wenchuan earthquake. Physica A: Stat. Mech. Appl. **390**(12), 2375–2380 (2011)